Supporting Information

pH-Controlled polymorphism in a layered dysprosium phosphonate and its impact on the magnetization relaxation

Dai Zeng, Min Ren, Song-Song Bao, Jian-Shen Feng, Li Li and Li-Min Zheng*

Experimental Section

    Materials and methods. 2-quinolinephosphonic acid was prepared according to the literature method[1] and all the other starting materials were obtained from commercial sources without further purification. Elemental analyses for C, H and N were determined with a Perkin Elmer 240C elemental analyzer. The Dy contents in the doped samples were analyzed using Inductively Coupled Plasma Optical Emission Spectrometry (ICP OES-Optima 5300DV, PE.). Infrared spectra were measured using KBr pellets on a Bruker Tensor 27 spectrometer in the range of 400-4000 cm^{-1}. Thermogravimetric analysis (TGA) were performed on a Mettler-Toledo TGA/DSC STARe thermal analyzer in the range of 25-600°C under a nitrogen flow at a heating rate of 5°C/min. Powder X-ray diffraction (PXRD) data were recorded on a Bruker D8 ADVANCE X-ray powder diffractometer (Cu-Kα) over the 2θ range of 5 to 50° at room temperature. The magnetic susceptibility data were recorded on a Quantum Design MPMS SQUID VSM system. The diamagnetic contribution of the sample itself was estimated from Pascal's constant.[2]

    Synthesis of α-Dy(C$_9$H$_6$NHPO$_3$)(SO$_4$)(H$_2$O)$_2$ (α-Dy): A mixture of Dy(NO$_3$)$_3$·6H$_2$O (0.0228 g, 0.05 mmol), ZnSO$_4$·6H$_2$O (0.0270 g, 0.10 mmol) and 2-quinolinephosphonic acid (0.0105 g, 0.05 mmol) in 6 mL of H$_2$O, adjusted to pH 1.50 with 1 mol/L H$_2$SO$_4$, was kept in a Teflon-lined autoclave at 140 °C for 2 days. After cooling to room temperature, white polycrystalline powders of **α-Dy** were obtained as a pure phase, confirmed by the powder XRD measurements. Yield: 60%. Elemental analysis calcd for α-C$_9$H$_{11}$DyNO$_9$PS: C, 21.50; H, 2.21; N, 2.79%. Found: C, 21.61; H, 2.48; N, 2.77%. IR (KBr, cm^{-1}): 3355 (br), 1639 (m), 1599 (w), 1518 (w), 1486 (w), 1445 (w), 1404 (w), 1383 (w), 1348 (w), 1294 (m), 1164 (s), 1138 (s), 1104 (s), 1041 (s), 970 (s), 883 (w), 855(w), 828 (m), 776 (w), 658 (s), 637 (s), 606 (s), 533 (m), 476 (m), 419 (w). Thermal

analysis shows a weight loss of 7.0% below 250°C, close to the calculated value for the release of two coordination water molecules (7.1%).

Synthesis of β-Dy(C₉H₆NHPO₃)(SO₄)(H₂O)₂ (β-Dy): $\beta\text{-Dy}(C_9H_6NHPO_3)(SO_4)(H_2O)_2$ (β-Dy): **β-Dy** was obtained following a similar procedure as that for **α-Dy** except that the pH was adjusted to 0.70. White polycrystalline powders of **β-Dy** were obtained as a pure phase, judged by the powder XRD measurements. Yield: 65%. Elemental analysis calcd for β-$C_9H_{11}DyNO_9PS$: C, 21.50; H, 2.21; N, 2.79%. Found: C, 21.54; H, 2.58; N, 2.78%. IR (KBr, cm^{-1}): 3479(m), 3356 (br), 3095 (w), 2355 (w), 1641 (m), 1599 (w), 1518 (w), 1486 (w), 1446 (w), 1405 (w), 1383 (w), 1348 (w), 1294 (m), 1167 (s), 1135 (s), 1103 (s), 1042 (s), 967 (s), 883 (w), 826 (m), 776 (w), 658 (s), 635 (s), 605 (s), 530 (m), 475 (m), 417 (w). Thermal analysis shows a weight loss of 7.4% below 250°C, close to the calculated value for the release of two coordination water molecules (7.1%).

Synthesis of α-Y(C₉H₆NHPO₃)(SO₄)(H₂O)₂ (α-Y): $\alpha\text{-Y}(C_9H_6NHPO_3)(SO_4)(H_2O)_2$ (α-Y): **α-Y** was obtained following a similar procedure as that for **α-Dy** except that Y(NO₃)₃·6H₂O (0.0192 g, 0.05 mmol) was used as the starting material instead of Dy(NO₃)₃·6H₂O. White polycrystalline powders were obtained as a pure phase, judged by the PXRD measurements. Yield: 55%. Elemental analysis calcd for α-$C_9H_{11}YNO_9PS$: C, 25.19; H, 2.58; N, 3.26%. Found: C, 25.03; H, 2.81; N, 3.17%. IR (KBr, cm^{-1}): 3484(m), 3356 (br), 3097 (w), 1643 (m), 1599 (w), 1520 (w), 1486 (w), 1445 (w), 1404 (w), 1384 (w), 1348 (w), 1294 (m), 1200 (s), 1167(s), 1135 (s), 1105 (s), 1044 (s), 971 (m), 949 (w), 885 (w), 856 (w), 828 (m), 781 (w), 769 (w), 660 (s), 637 (s), 608 (s), 593 (m), 534 (m), 476 (w), 418 (w). Thermal analysis shows a weight loss of 8.6% below 250°C, close to the calculated value for the release of two coordination water molecules (8.4%).

Synthesis of β-Y(C₉H₆NHPO₃)(SO₄)(H₂O)₂ (β-Y): $\beta\text{-Y}(C_9H_6NHPO_3)(SO_4)(H_2O)_2$ (β-Y): **β-Y** was obtained following a similar procedure as that for **β-Dy** except that Y(NO₃)₃·6H₂O (0.0192 g, 0.05 mmol) was used as the starting material instead of Dy(NO₃)₃·6H₂O. White polycrystalline powders were obtained as a pure phase, judged by the PXRD measurements. Yield: 42%. Elemental analysis calcd for β-$C_9H_{11}YNO_9PS$: C, 25.19; H, 2.58; N, 3.26%. Found: C, 25.12; H, 2.80; N, 3.20%. IR (KBr, cm^{-1}): 3486(m), 3306 (br), 1643 (m), 1599 (w), 1519 (w), 1486 (w), 1445 (w), 1404 (w), 1384 (w), 1347 (w), 1294 (w), 1200 (s), 1173(s), 1133 (s), 1105 (s), 1044 (s), 967 (m), 949 (w), 884 (w), 855 (w), 823 (m), 781 (w), 769

(w), 659 (m), 636 (m), 608 (m), 593 (m), 533 (m), 475 (w), 430 (w), 416 (w). Thermal analysis shows a weight loss of 8.7% below 250°C, close to the calculated value for the release of two coordination water molecules (8.4%).

Synthesis of α-Dy$_{0.10}$Y$_{0.90}$(C$_9$H$_6$NHPO$_3$)(SO$_4$)(H$_2$O)$_2$ (α-Dy$_{0.10}$Y$_{0.90}$): A mixture of Dy(NO$_3$)$_3$·6H$_2$O (0.0045 g, 0.01 mmol), Y(NO$_3$)$_3$·6H$_2$O (0.0345 g, 0.09 mmol), ZnSO$_4$·6H$_2$O (0.0270 g, 0.1 mmol) and 2-quinolinephosphonic acid (0.0105 g, 0.05 mmol) in 6 mL of H$_2$O, adjusted to pH 1.50 with 1 mol/L H$_2$SO$_4$, was kept in a Teflon-lined autoclave at 140 °C for 2 days. White polycrystalline powders were obtained after cooling to room temperature. Yield: 70%. Elemental analysis calcd for α-C$_9$H$_{11}$Dy$_{0.103}$Y$_{0.897}$NO$_9$PS: C, 24.75; H, 2.54; N, 3.21%. Found: C, 24.78; H, 3.02; N, 3.21 %. IR (KBr, cm^{-1}): 3388 (br), 3097 (w), 1640 (m), 1600 (w), 1518 (w), 1486 (w), 1446 (w), 1404 (w), 1384 (w), 1348 (w), 1295 (w), 1165 (s), 1139 (s), 1106 (s), 1044 (s), 972 (s), 883 (w), 854(w), 828 (m), 776 (w), 660 (s), 637 (s), 606 (s), 534 (m), 475 (w), 420 (w). The amount of Dy^{III} in **α-Dy$_{0.10}$Y$_{0.90}$** (10.3 %) is confirmed by the inductively coupled plasma (ICP) measurements.

Synthesis of β-Dy$_{0.12}$Y$_{0.88}$(C$_9$H$_6$NHPO$_3$)(SO$_4$)(H$_2$O)$_2$ (β-Dy$_{0.12}$Y$_{0.88}$): A mixture of Dy(NO$_3$)$_3$·6H$_2$O (0.0045 g, 0.01 mmol), Y(NO$_3$)$_3$·6H$_2$O (0.0345 g, 0.09 mmol), ZnSO$_4$·6H$_2$O (0.0270 g, 0.1 mmol) and 2-quinolinephosphonic acid (0.0105 g, 0.05 mmol) in 6 mL of H$_2$O, adjusted to pH 0.70 with 1 mol/L H$_2$SO$_4$, was kept in a Teflon-lined autoclave at 140 °C for 2 days. White polycrystalline powders were obtained after cooling to room temperature. Yield: 57%. Elemental analysis calcd for β-C$_9$H$_{11}$Dy$_{0.12}$Y$_{0.88}$NO$_9$PS: C, 24.68; H, 2.53; N, 3.20%. Found: C, 24.95; H, 2.69; N, 3.24%. IR (KBr, cm^{-1}): 3486(s), 3298 (br), 1644 (m), 1599 (w), 1519 (w), 1488 (w), 1446 (w), 1403 (w), 1384 (w), 1346 (w), 1295 (w), 1199 (s), 1175 (s), 1143 (s), 1131 (s), 1104 (s), 1045 (s), 966 (m), 927 (w), 884 (w), 854(w), 843 (w), 821 (w), 780 (w), 768 (w), 665 (w), 634 (m), 607 (m), 592 (m), 532 (m), 492(w), 475 (w), 415(w). The amount of Dy^{III} in β-**DyY** (11.7%) is confirmed by the inductively coupled plasma (ICP) measurements.

Single-Crystal Structure Determination. Single crystals of dimensions 0.20 × 0.20 × 0.05 mm^3 for **α-Dy**, 0.10 × 0.05 × 0.05 mm^3 for **β-Dy** and 0.10 × 0.05 × 0.05 mm^3 for **β-Y** were mounted on a glass rod. The crystal data were collected on a Bruker SMART APEX II diffractometer using monochromated Mo-Kα radiation (λ = 0.71073 Å) at 296

K for **α-Dy**, **β-Dy** and **β-Y**. The structures were solved by direct methods and refined on F^2 by full matrix least squares using SHELXTL.[3] All non-hydrogen atoms were refined anisotropically. All hydrogen atoms were either put in calculated positions or found from the difference Fourier maps and refined isotropically. Selected bond lengths and angles are given in Table S1.

The Cole-Cole plot fitting method: The *ac* magnetic susceptibilities can be described by the Cole-Cole plots using the generalized Debye model in Eq(S1), Eq(S2)[4] (single relaxation model) and/or a linear combination of two modified Debye models, as shown in Eq(S3) and Eq(S4)[5] (double relaxation model):

$$\chi'(\omega) = \chi_S + \frac{(\chi_T - \chi_S)\left[1 + (\omega\tau)^{1-\alpha} \sin(\pi\alpha/2)\right]}{1 + 2(\omega\tau)^{1-\alpha} \sin(\pi\alpha/2) + (\omega\tau)^{2(1-\alpha)}} \quad (S1)$$

$$\chi''(\omega) = \frac{(\chi_T - \chi_S)\left[1 + (\omega\tau)^{1-\alpha} \cos(\pi\alpha/2)\right]}{1 + 2(\omega\tau)^{1-\alpha} \sin(\pi\alpha/2) + (\omega\tau)^{2(1-\alpha)}} \quad (S2)$$

$$\chi'(\omega) = \chi_S + (\chi_T - \chi_S)\left(\frac{f_A\left[1 + (\omega\tau_A)^{1-\alpha_A} \sin(\pi\alpha_A/2)\right]}{1 + 2(\omega\tau_A)^{1-\alpha_A} \sin(\pi\alpha_A/2) + (\omega\tau_A)^{2(1-\alpha_A)}} + \frac{(1 - f_A)\left[1 + (\omega\tau_B)^{1-\alpha_B} \sin(\pi\alpha_B/2)\right]}{1 + 2(\omega\tau_B)^{1-\alpha_B} \sin(\pi\alpha_B/2) + (\omega\tau_B)^{2(1-\alpha_B)}}\right) \quad (S3)$$

$$\chi'(\omega) = (\chi_T - \chi_S)\left(\frac{f_A\left[1 + (\omega\tau_A)^{1-\alpha_A} \cos(\pi\alpha_A/2)\right]}{1 + 2(\omega\tau_A)^{1-\alpha_A} \sin(\pi\alpha_A/2) + (\omega\tau_A)^{2(1-\alpha_A)}} + \frac{(1 - f_A)\left[1 + (\omega\tau_B)^{1-\alpha_B} \cos(\pi\alpha_B/2)\right]}{1 + 2(\omega\tau_B)^{1-\alpha_B} \sin(\pi\alpha_B/2) + (\omega\tau_B)^{2(1-\alpha_B)}}\right) \quad (S4)$$

where χ_S is the adiabatic susceptibility, χ_T is the isothermal susceptibility, and τ is the average relaxation time of magnetization, and the α parameter, which ranges between 0 and 1, quantifies the width of the τ distribution, f_A represents the percentage of relaxation A.

References:

1. C. Xu, B. Liu, S.-S. Bao, Y. Chen, L.-M. Zheng, *Solid State Sci.*, 2007, **9**, 686-692.
2. O. Kahn*, Molecular Magnetism,* VCH Publishers, Inc., New York, **1993**.
3. SHELXTL (version 5.0), Reference Manual, Siemens Industrial Automation, Analytical Instruments Madison, WI, 1995.
4. D. Gatteschi, R. Sessoli, J.Villain, *Molecular Nanomagnets*, Oxford University, New York, 2006.
5. N. Domingo, F. Luis, M. Nakano, M. Muntó, J. Gómez, J. Chaboy, N. Ventosa, J. Campo, J. Veciana, D. Ruiz-Molina, *Phys Rev B* 2009, **79**, 214404

Table S1. Crystal data for compounds **α-Dy**, **β-Dy** and **β-Y**.

	α-Dy	β-Dy	β-Y
Formula	$C_9H_{11}DyNO_9PS$	$C_9H_{11}DyNO_9S$	$C_9H_{11}NO_9PSY$
Fw	502.72	502.72	429.13
crystal size	0.08×0.20×0.40	0.05×0.05×0.10	0.05×0.05×0.10
Temperature (K)	296	296	296
crystal system	monoclinic	triclinic	triclinic
Space group	$P2_1/c$	$P\bar{1}$	$P\bar{1}$
a (Å)	13.3163(5)	6.792(3)	6.778(3)
b (Å)	6.7704(3)	7.596(4)	7.572(3)
c (Å)	15.0967(6)	13.368(6)	13.356(5)
α (°)		90.362(8)	90.423(6)
β (°)	90.6391(6)°	93.280(7	93.298(7)
γ (°)		102.383(7)	102.310(6)
V (Å^3)	1360.98(10)	672.4(5)	668.4(4)
Z	4	2	2
D_c (g cm^{-3})	2.454	2.483	2.132
μ (mm^{-1})	5.809	5.879	4.687
F (000)	964	482	428
R_1, wR_2[a] [$I > 2\sigma(I)$]	0.0170, 0.0405	0.0354, 0.0910	0.0601, 0.1378
R_1, wR_2[a] (all data)	0.0188, 0.0415	0.0390, 0.0936	0.0885, 0.1533
goodness-of-fit	1.01	1.01	1.01
$(\Delta\rho)_{max}$, $(\Delta\rho)_{min}$ (e Å^{-3})	1.10, -0.58	3.48, -1.29	1.76, -1.06
CCDC number	1035243	1035242	1035244

[a]$R_1 = \Sigma||F_o|-|F_c||/\Sigma|F_o|$. $wR_2 = [\Sigma w(F_o^2-F_c^2)^2/\Sigma w(F_o^2)^2]^{1/2}$

Table S2. Selected bond lengths (Å) and angles (deg) for compounds **α-Dy**, **β-Dy** and **β-Y**.

	α-Dy	**β-Dy**	**β-Y**	
Dy1-O1	2.292(2)	2.287(4)	Y1-O1	2.271(4)
Dy1-O4	2.423(2)	2.440(4)	Y1-O4	2.436(4)
Dy1-O5	2.472(2)	2.449(4)	Y1-O5	2.435(4)
Dy1-O2A	2.255(2)	2.265(4)	Y1-O2A	2.256(4)
Dy1-O3B	2.312(2)	2.337(4)	Y1-O3B	2.333(4)
Dy1-O5C	2.425(2)	2.482(4)	Y1-O5C	2.484(4
Dy1-O1W	2.420(2)	2.420(4)	Y1-O1W	2.402(5)
Dy1-O2W	2.437(2)	2.420(4)	Y1-O2W	2.409(4)
O1-Dy1-O1W	79.97(7)	79.11(15)	O1-Y1-O1W	79.26(14)
O1-Dy1-O2W	75.82(8)	74.09(15)	O1-Y1-O2W	74.09(15)
O1-Dy1-O4	162.42(8)	162.95(14)	O1-Y1-O4	162.87(15)
O1-Dy1-O5	138.45(7)	139.61(13)	O1-Y1-O5	139.63(14)
O1-Dy1-O2A	87.88(8)	97.25(15)	O1-Y1-O2A	97.21(16)
O1-Dy1-O3B	105.48(7)	96.11(15)	O1-Y1-O3B	96.21(16)
O1-Dy1-O5C	78.94(7)	77.41(13)	O1-Y1-O5C	77.36(14)
O1W-Dy1-O2W	140.06(8)	130.12(14)	O1W-Y1-O2W	129.94(15)
O1W-Dy1-O4	87.97(7)	84.25(13)	O1W-Y1-O4	83.99(14)
O1W-Dy1-O5	139.82(7)	140.63(13)	O1W-Y1-O5	140.45(14)
O1W-Dy1-O2A	74.74(8)	74.18(14)	O1W-Y1-O2A	74.43(16)
O1W-Dy1-O3B	72.23(7)	73.91(14)	O1W-Y1-O3B	73.28(15)
O1W-Dy1-O5C	133.42(7)	140.37(13)	O1W-Y1-O5C	140.59(14)
O2W-Dy1-O4	106.70(8)	115.09(15)	O2W-Y1-O4	115.08(15)
O2W-Dy1-O5	74.75(7)	79.48(14)	O2W-Y1-O5	79.67(14)
O2W-Dy1-O3B	145.01(7)	68.18(13)	O2W-Y1-O3B	68.53(14)
O2W-Dy1-O2A	73.10(8)	149.62(14)	O2W-Y1-O2A	149.61(15)
O2W-Dy1-O5C	71.80(7)	72.06(13)	O2W-Y1-O5C	72.15(14)
O4-Dy1-O5	56.90(7)	57.41(12)	O4-Y1-O5	57.47(14)
O4-Dy1-O2A	76.56(9)	81.52(15)	O4-Y1-O2A	81.60(15)
O4-Dy1-O3B	82.61(8)	75.63(14)	O4-Y1-O3B	75.36(15)
O4-Dy1-O5C	118.55(7)	118.54(13)	O4-Y1-O5C	118.67(14)
O5-Dy1-O2A	110.52(8)	90.33(14)	O5-Y1-O2A	90.15(15)
O5-Dy1-O3B	83.47(7)	101.81(13)	O5-Y1-O3B	102.11(14)
O5-Dy1-O5C	64.38(6)	65.56(15)	O5-Y1-O5C	65.57(13)
O2A-Dy1-O3B	141.28(8)	142.20(14)	O2A-Y1-O3B	141.86(14)
O3B-Dy1-O5C	74.18(7)	139.94(13)	O3B-Y1-O5C	140.38(14)
O2A-Dy1-O5C	144.54(8)	77.65(14)	O2A-Y1-O5C	77.56(14)
Dy1-O5-Dy1C	115.62(8)	114.435(11)	Y1-O5-Y1C	114.43(16)

Symmetry transformations used to generate equivalent atoms for **α-Dy**: A: -x+1, y+1/2, -z+1/2; B: -x+1, y-1/2, -z+1/2; C: -x+1, -y, -z+1. For **β-Dy** and **β-Y**: A: -x+1, -y+1, -z+1; B: -x, -y+1, -z+1; C: -x+1, -y+2, -z+1.

Table S3. Hydrogen bond lengths (Å) and angles (deg) for compounds **α-Dy** and **β-Dy**.

	D-H···A	d(D-H)	d(H···A)	d(D···A)	∠ DHA
α-Dy[a]	O1W-H1Wa···O1[iii]	0.8500	2.1100	2.898(3)	154.00
	O1W-H1Wb···O6[iv]	0.8500	1.9800	2.765(4)	153.00
	O2W-H2Wa···O7[ii]	0.8500	2.3700	2.946(4)	125.00
	O2W-H2Wb···O3[i]	0.8500	2.0500	2.831(3)	151.00
	N1-H1a···O7[ii]	0.8600	1.9300	2.758(4)	160.00
	C5-H5···O6[v]	0.9300	2.5100	3.312(4)	145.00
	C6-H6···O4[vi]	0.9300	2.5100	3.143(5)	126.00
β-Dy[b]	O1W-H1Wa···O6[ii]	0.8600	1.8600	2.711(6)	169.00
	O1W-H1Wb···O1[i]	0.8600	2.2000	2.909(6)	139.00
	O2W-H2Wa···O7[iv]	0.8600	2.4200	2.714(6)	101.00
	O2W-H2Wb···O2[iii]	0.8600	2.4400	3.243(6)	155.00
	N1-H1a···O7[iv]	0.8600	1.9800	2.799(6)	160.00
	C5-H5···O6[v]	0.9300	2.4400	3.234(9)	143.00
	C6-H6···O4[vi]	0.9300	2.4900	3.164(8)	129.00

[a]Symmetry codes: i, x, 1/2-y, 1/2+z; ii, 1-x, -y, 1-z; iii, 1-x, -1/2+y, 1/2-z; iv, x, 1/2-y, -1/2+z; v, 1+x, 1/2-y, -1/2+z; vi, 1+x, y, z.
[b]Symmetry codes: i, -x, 1-y, 1-z; ii, x, -1+y, z; iii, x, 1+y, z; iv, 1-x, 2-y, 1-z; v, x, -1+y, 1+z; vi, x, y, 1+z.

Table S4. The parameters obtained by fitting the χ_M'' versus frequency data for compound **α-Dy** in different *dc* fields at 5 K.

H / kOe	χ_T / cm³·mol⁻¹	χ_S / cm³·mol⁻¹	$\ln(\tau_A$ / s)	α_A	$\ln(\tau_B$ / s)	α_B	f_A	R[a]
1.0	2.31	1.65	-4.17	0.20	-9.47	0.24	0.19	4.2×10^{-6}
1.5	2.21	1.19	-3.72	0.17	-8.79	0.33	0.18	3.1×10^{-5}
2.0	2.14	0.95	-3.63	0.29	-8.39	0.31	0.28	8.1×10^{-6}
2.5	2.06	0.76	-3.45	0.28	-8.24	0.32	0.34	2.5×10^{-5}
3.0	2.02	0.64	-3.19	0.34	-8.24	0.30	0.45	1.3×10^{-5}

[a]$R = \sum[(\chi'_{obs} - \chi'_{cal})^2 + (\chi''_{obs} - \chi''_{cal})^2] / \sum[\chi'_{obs}{}^2 + \chi''_{obs}{}^2]$

Table S5. The parameters obtained by fitting the χ_M'' versus frequency data for compound **α-Dy** under 2 kOe *dc* field.

T/K	χ_T/ cm^3·mol^{-1}	χ_S/ cm^3·mol^{-1}	$\ln(\tau_B/$s)	α_B	$\ln(\tau_A/$s)	α_A	f_B	R^b
2.0	0.20	0.02	-0.48	0.20	-8.21	0.46	0.72	2.6×10^{-4}
2.5	0.20	0.02	-1.09	0.14	-8.11	0.55	0.66	2.6×10^{-5}
3.0	0.20	0.02	-1.47	0.19	-8.14	0.56	0.61	1.7×10^{-4}
3.5	0.17	0^a	-2.15	0.07	-7.84	0.72	0.31	3.2×10^{-4}
4.0	0.16	0.02	-2.35	0.30	-8.09	0.55	0.47	1.2×10^{-5}
4.5	0.14	0.03	-3.05	0.30	-8.09	0.42	0.45	2.9×10^{-5}
5.0	0.12	0.03	-3.46	0.26	-8.33	0.38	0.37	2.6×10^{-5}
6.0	0.10	0.03	-4.42	0.34	-8.92	0.18	0.36	2.3×10^{-5}
7.0	0.08	0.04	-5.91	0.28	-9.36	0.06	0.31	7.6×10^{-6}
8.0	0.07	0.03			-9.97	0.47		1.9×10^{-5}
9.0	0.06	0.03			-10.59	0.33		1.7×10^{-5}
10.0	0.06	0.03			-10.98	0.18		1.7×10^{-6}

^{a} This parameter value is fixed to zero. $^b R = \sum[(\chi'_{obs} - \chi'_{cal})^2 + (\chi''_{obs} - \chi''_{cal})^2]\,/\,\sum[\chi'^2_{obs} + \chi''^2_{obs}]$

Table S6. The parameters obtained by fitting the χ_M'' versus frequency data for compound **α-Dy$_{0.10}$Y$_{0.90}$** under 2 kOe *dc* field.

T/K	χ_T/ cm^3·mol^{-1}	χ_S/ cm^3·mol^{-1}	$\ln(\tau/$s)	α	R^a
2.0	0.016	0.001	-4.32	0.39	2.4×10^{-4}
2.5	0.015	0.001	-4.53	0.40	2.7×10^{-4}
3.0	0.013	0.001	-4.81	0.39	1.9×10^{-4}
3.5	0.011	0.002	-5.13	0.37	2.4×10^{-4}
4.0	0.010	0.002	-5.48	0.36	1.3×10^{-4}
4.5	0.009	0.002	-5.89	0.34	7.7×10^{-5}
5.0	0.008	0.002	-6.30	0.33	7.9×10^{-4}
6.0	0.007	0.002	-7.19	0.31	4.8×10^{-5}
7.0	0.006	0.002	-7.97	0.32	6.5×10^{-5}
8.0	0.005	0.003	-8.46	0.25	2.8×10^{-5}
9.0	0.005	0.003	-8.75	0.23	3.4×10^{-5}
10.0	0.004	0.003	-9.25	0.30	2.0×10^{-5}

$^a R = \sum[(\chi'_{obs} - \chi'_{cal})^2 + (\chi''_{obs} - \chi''_{cal})^2]\,/\,\sum[\chi'^2_{obs} + \chi''^2_{obs}]$

Table S7. The parameters obtained by fitting the χ_M'' versus frequency data for compound **β-Dy** under 2 kOe *dc* field.

T/K	χ_T/ cm^3·mol^{-1}	χ_S/ cm^3·mol^{-1}	$\ln(\tau/$ s$)$	α	R^{a}
3.5	0.20	0.01	-4.90	0.59	1.4×10^{-5}
4.0	0.19	0.01	-5.02	0.59	7.7×10^{-5}
4.5	0.18	0.01	-5.04	0.57	1.4×10^{-4}
5.0	0.16	0.01	-5.27	0.55	1.3×10^{-3}
6.0	0.13	0.03	-5.72	0.33	2.3×10^{-4}
7.0	0.11	0.03	-6.43	0.25	7.5×10^{-4}
8.0	0.09	0.03	-7.52	0.17	5.0×10^{-5}
9.0	0.08	0.02	-8.80	0.12	8.8×10^{-4}
10.0	0.07	0.02	-9.98	0.03	3.6×10^{-5}

$^{\text{a}}R = \sum[(\chi'_{obs} - \chi'_{cal})^2 + (\chi''_{obs} - \chi''_{cal})^2] / \sum[\chi'_{obs}{}^2 + \chi''_{obs}{}^2]$

Table S8. The parameters obtained by fitting the χ_M'' versus frequency data for compound **β-Dy$_{0.12}$Y$_{0.88}$** under zero *dc* field.

T/K	χ_T/ cm^3·mol^{-1}	χ_S/ cm^3·mol^{-1}	$\ln(\tau/$ s$)$	α	R^{a}
6	2.65	1.35	-6.07	0.26	8.0×10^{-5}
7	2.27	0.90	-7.24	0.25	2.0×10^{-4}
8	1.96	0.84	-8.27	0.11	7.4×10^{-5}
9	1.74	0.78	-9.60	0.08	5.3×10^{-5}
10	1.56	1.16	-10.50	0.12	1.6×10^{-5}

Table S9. The parameters obtained by fitting the χ_M'' versus frequency data for compound **β-Dy$_{0.10}$Y$_{0.90}$** under 2 kOe *dc* field.

T/K	χ_T/ cm^3·mol^{-1}	χ_S/ cm^3·mol^{-1}	$\ln(\tau/$ s$)$	α	R^{a}
2	6.94	0.16	-0.96	0.41	5.0×10^{-3}
3	6.5	0.23	-0.83	0.40	5.6×10^{-3}
4	5.02	0.22	-1.34	0.36	5.2×10^{-3}
5	3.39	0.26	-2.75	0.20	3.0×10^{-3}
6	2.54	0.26	-4.28	0.10	2.5×10^{-3}
7	2.19	0.26	-5.86	0.07	9.7×10^{-4}
8	1.93	0.28	-7.52	0.07	4.5×10^{-4}
9	1.71	0.29	-9.23	0.10	1.1×10^{-4}
10	1.55	0.80	-10.56	0.21	7.3×10^{-5}
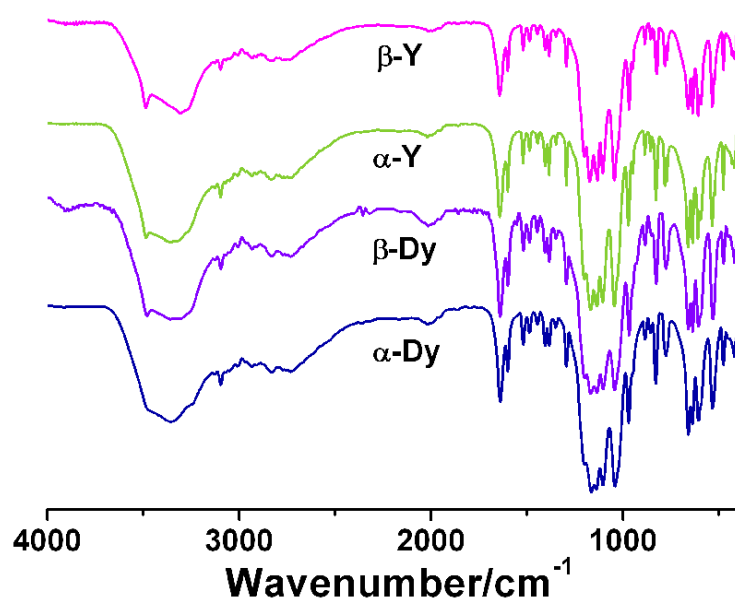
Figure S1. IR spectra for for **α-Dy**, **α-Y**, **β-Dy** and **β-Y**.
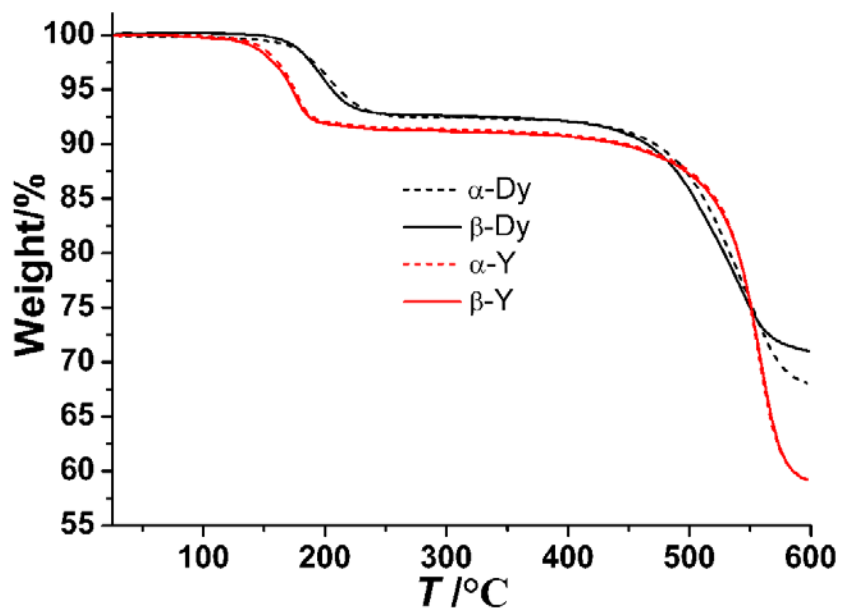
Figure S2. TG curves for **α-Dy**, **α-Y**, **β-Dy** and **β-Y**.

(a)

(b)
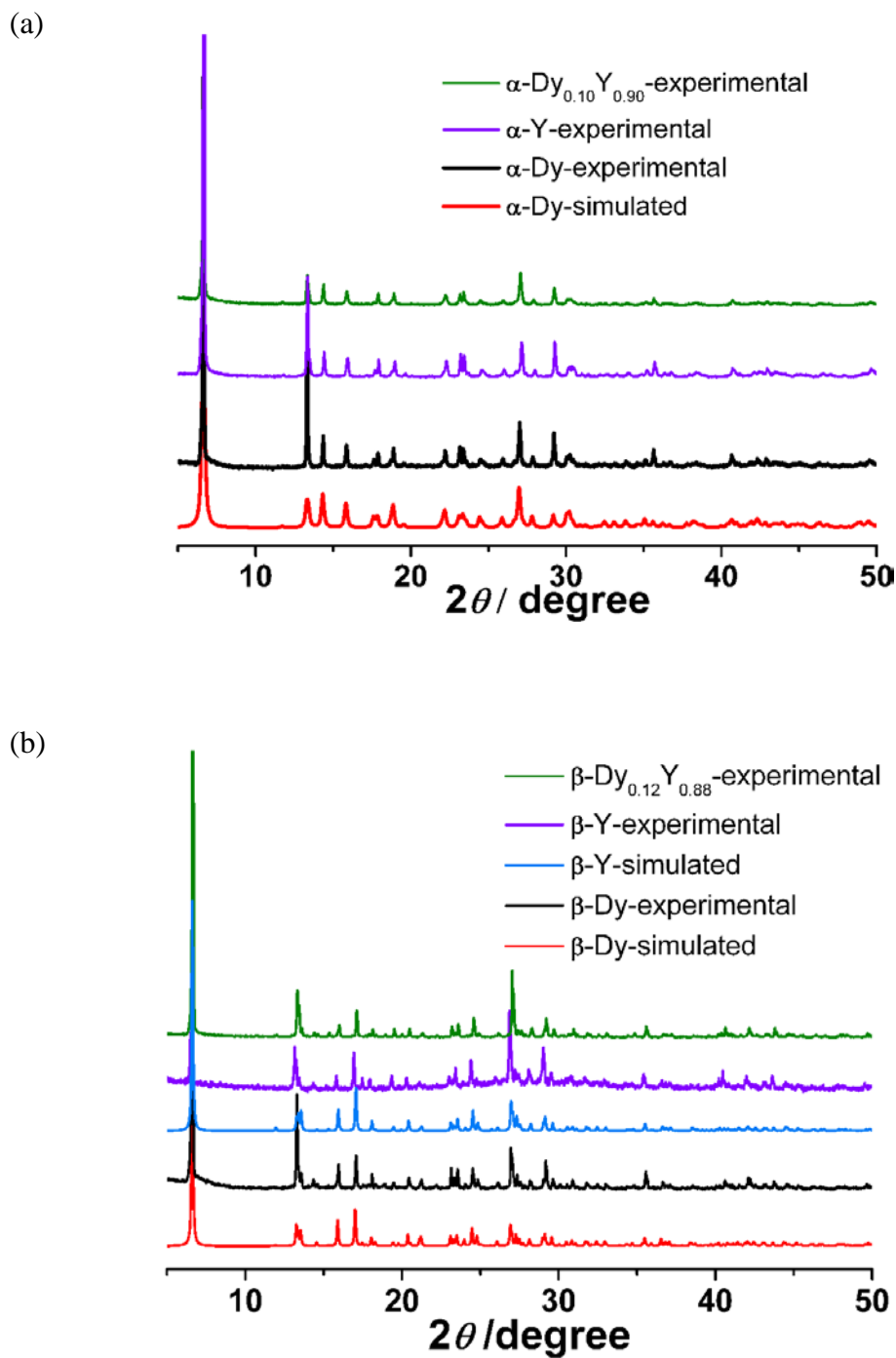
Figure S3. The powder XRD patterns for compounds **α-Dy**, **α-Y**, **α-Dy$_{0.10}$Y$_{0.90}$** (a) and **β-Dy, β-Y, β-Dy$_{0.12}$Y$_{0.88}$** (b). The patterns simulated from the single crystal data of **α-Dy** and **β-Dy** are also given.
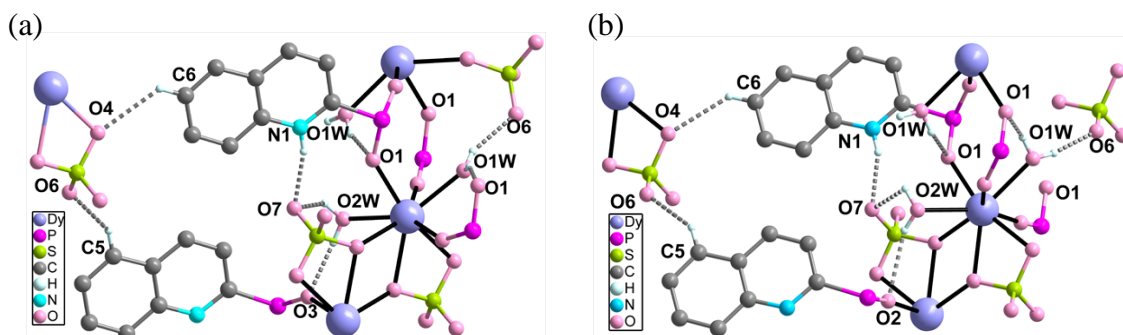
Figure S4. Intra- and inter-layer hydrogen-bond interactions in **α-Dy** (a) and **β-Dy** (b).
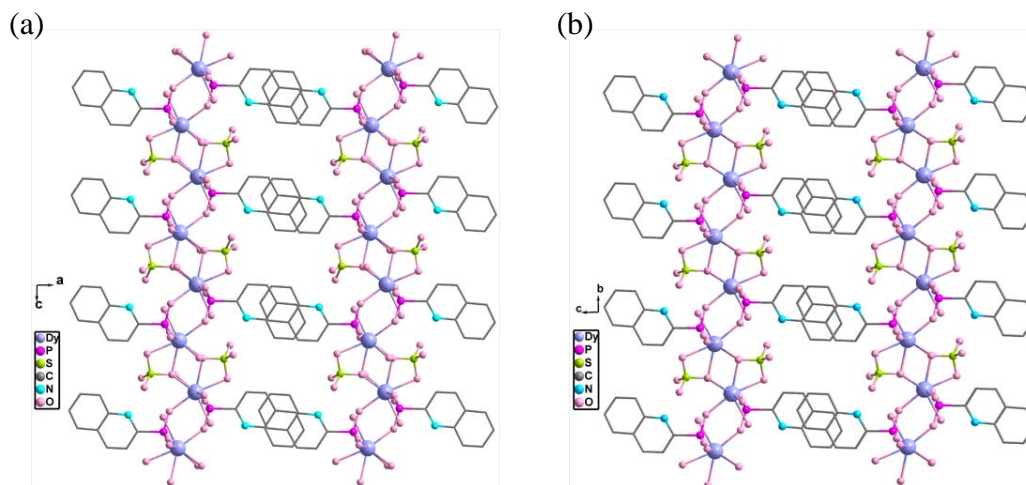
Figure S5. Packing diagrams of structures **α-Dy** viewed along the *b*-axis (a), and **β-Dy** viewed along the *a*-axis (b). All H atoms are omitted for clarity.
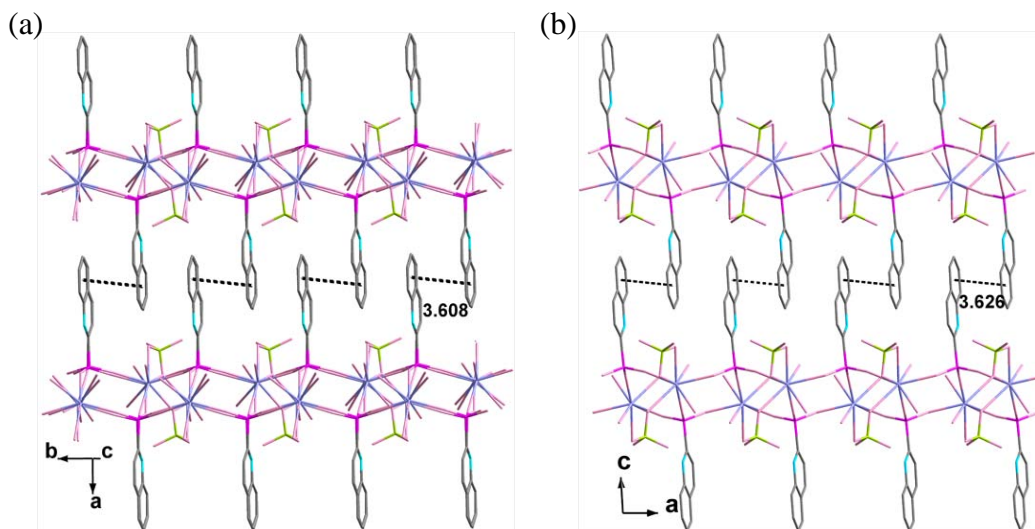
Figure S6. The inter-layer π-π stackings in structures **α-Dy** (a) and **β-Dy** (b).
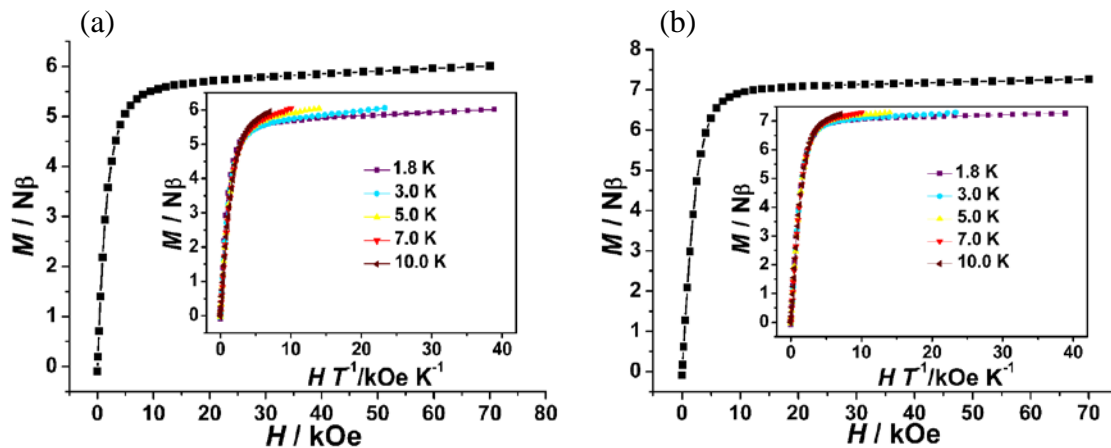
Figure S7. Field dependence of magnetization for **α-Dy** (a) and **β-Dy** (b) measured at 1.8 K. Inset: M vs. H/T plots for **α-Dy** (a) and **β-Dy** (b) at indicated temperatures.
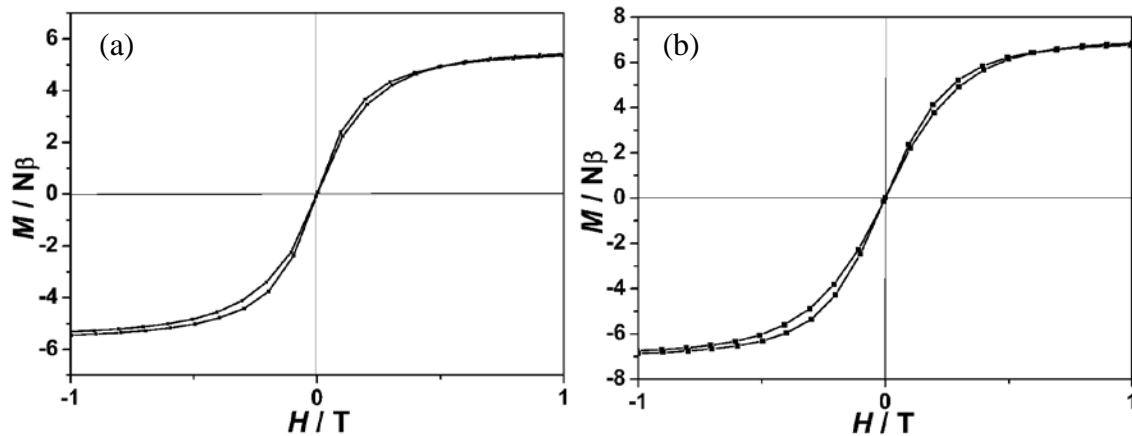
Figure S8. Hysteresis loops for **α-Dy** (a) and **β-Dy** (b) measured at 1.8 K with a sweep rate of 500 Oe/s.
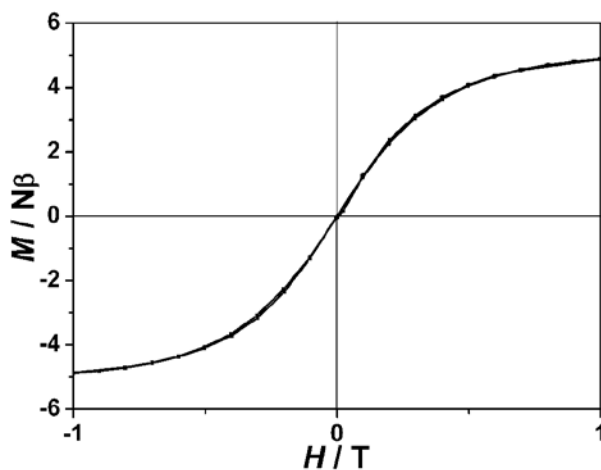
Figure S9. Hysteresis loop for **α-Dy$_{0.10}$Y$_{0.90}$** at 1.8 K with a sweep rate of 500 Oe/s.
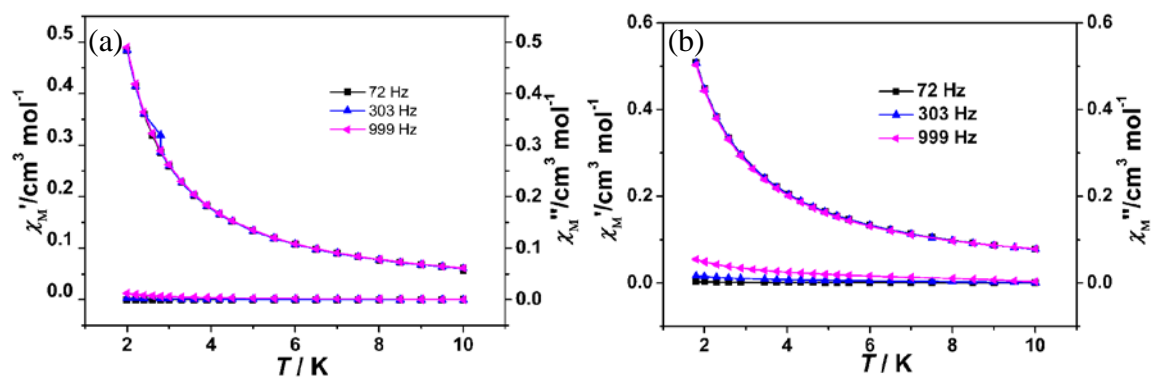
Figure S10. Temperature dependent in-phase (χ_M') and out-of-phase (χ_M'') signals for compounds **α-Dy** (a) and **β-Dy** (b) at zero *dc* field.
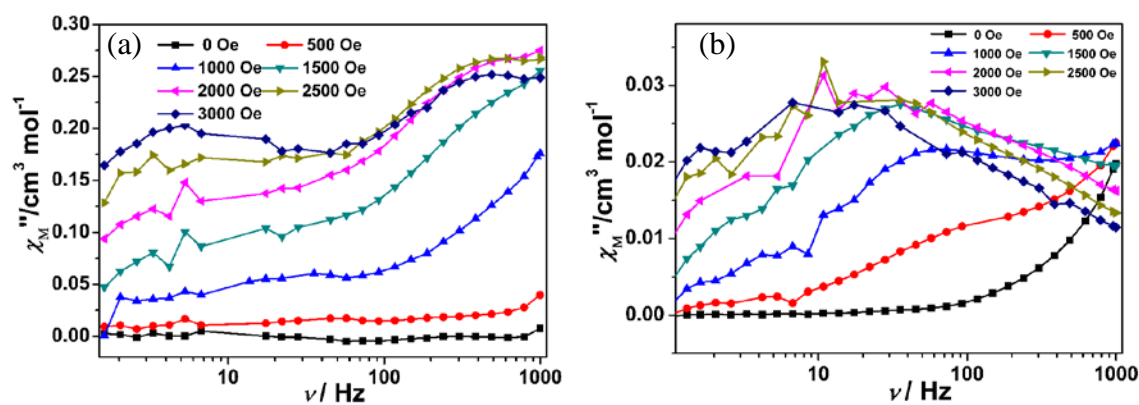
Figure S11. Frequency dependence of the out-of-phase susceptibilities of compounds **α-Dy** (a) and **β-Dy** (b) at 5 K under different *dc* fields.
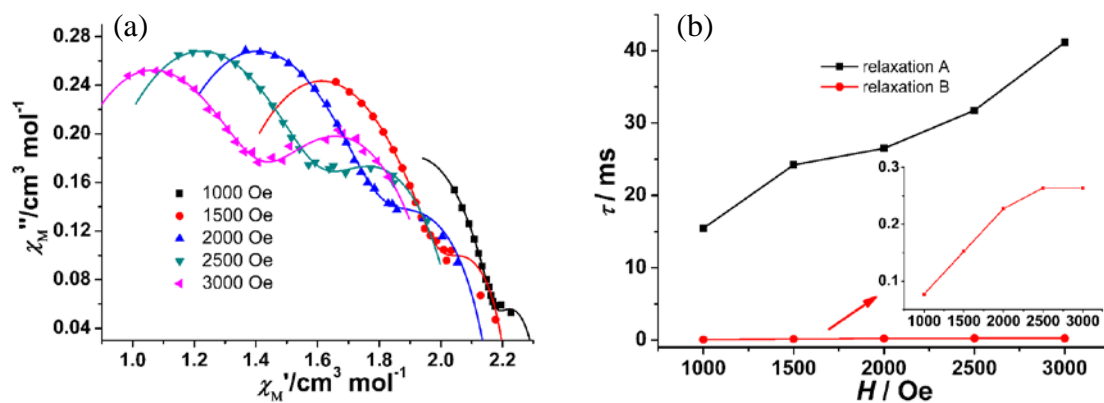

Figure S12. (a) Cole-Cole plots for **α-Dy** obtained using the *ac* susceptibility data at 5 K under different *dc* fields. (b) Field dependent magnetic relaxation time at 5 K for **α-Dy**.
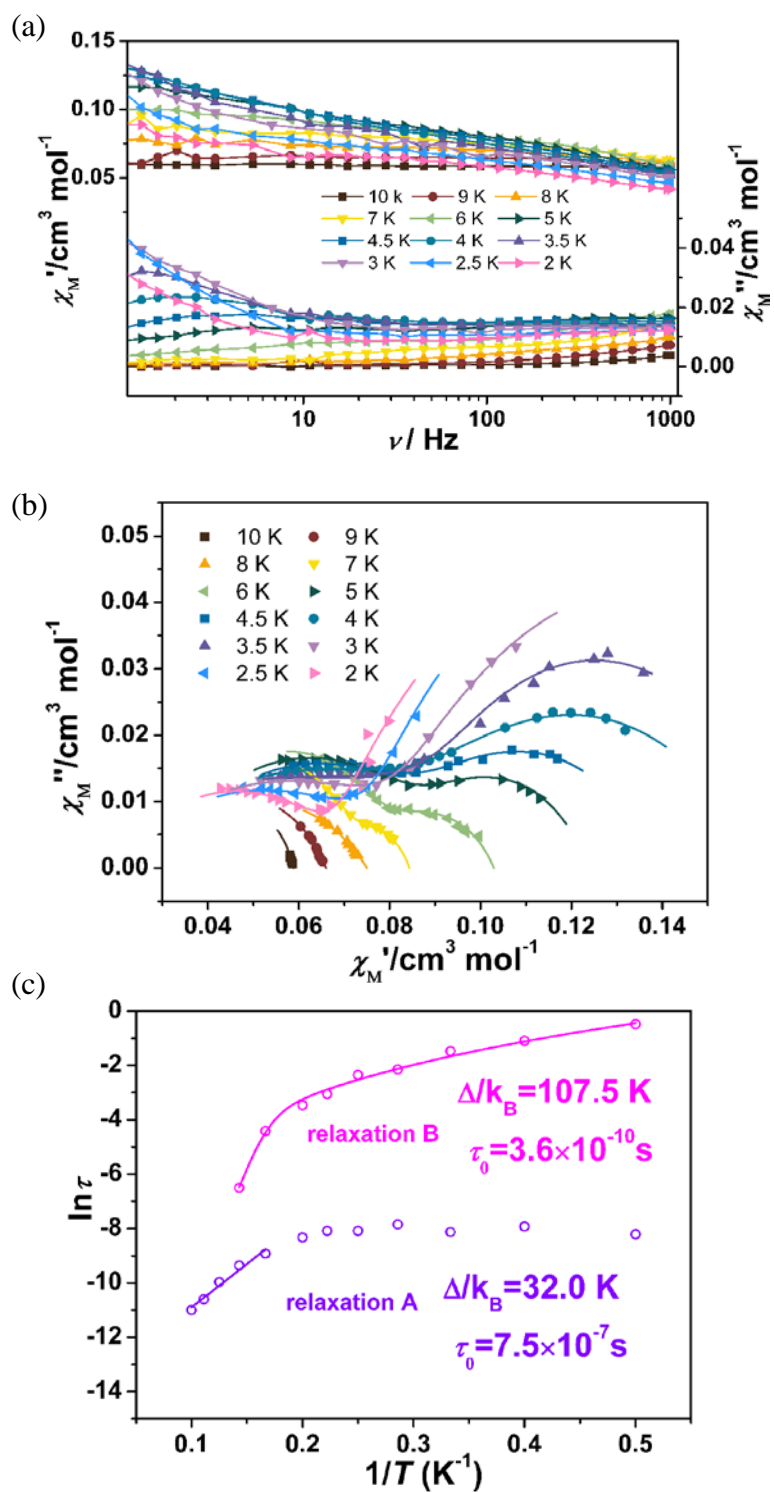
Figure S13. The χ_M' and χ_M'' versus frequency plots (a), Cole-Cole plots (b) and $\ln(\tau)$ versus T^{-1} plots for **α-Dy** under 2 kOe *dc* field. The solid lines are either eye-guided (a) or best fits (b, c).
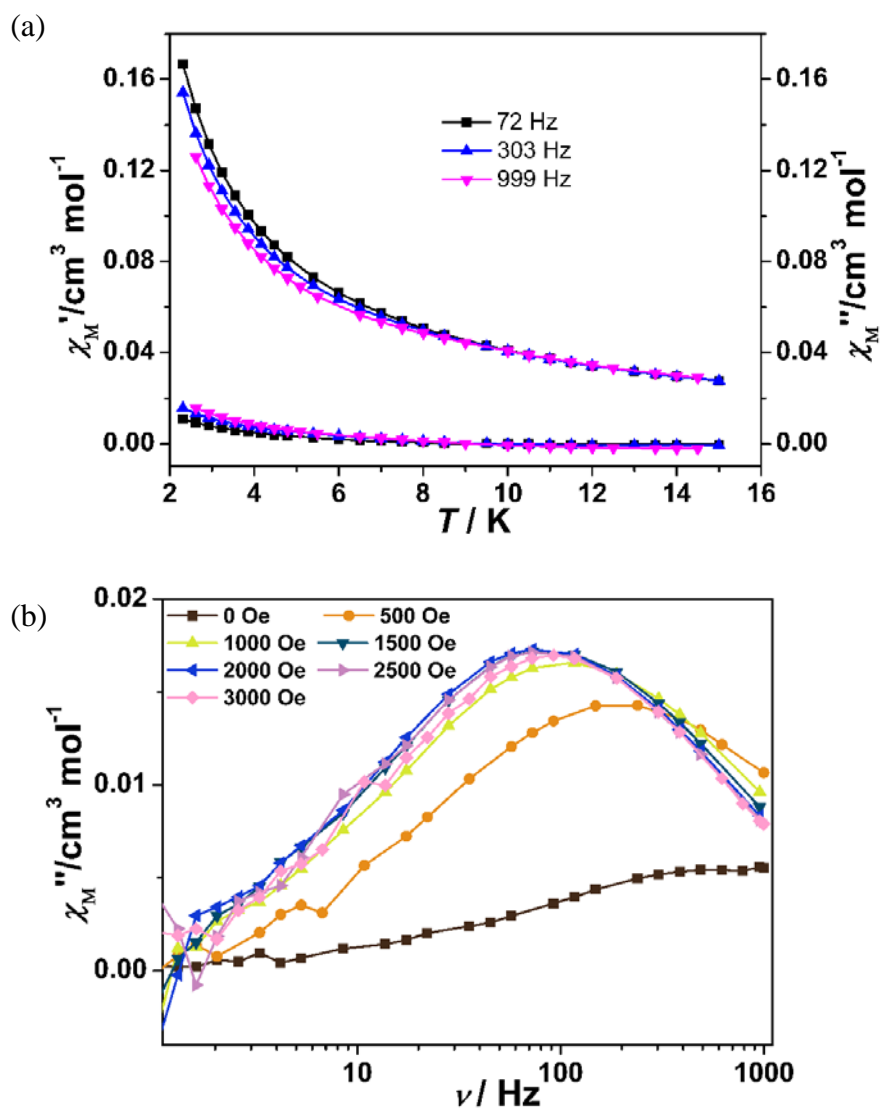
Figure S14. (a) Temperature dependent in-phase (χ_M') and out-of-phase (χ_M'') signals for compound **α-Dy$_{0.10}$Y$_{0.90}$** under zero *dc* field. (b) Frequency dependence of the out-of-phase susceptibility of compound **α-Dy$_{0.10}$Y$_{0.90}$** at 5 K under different *dc* fields.
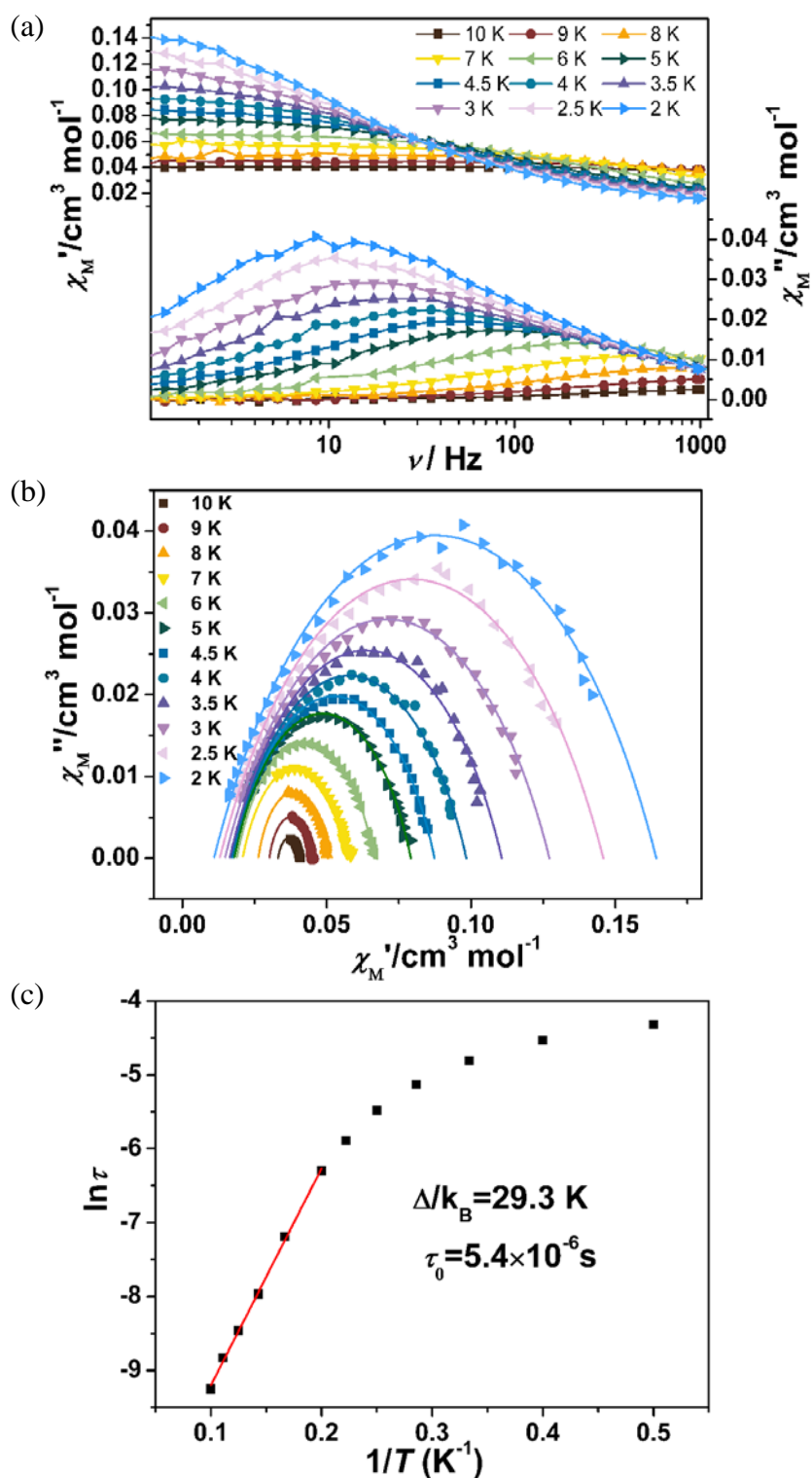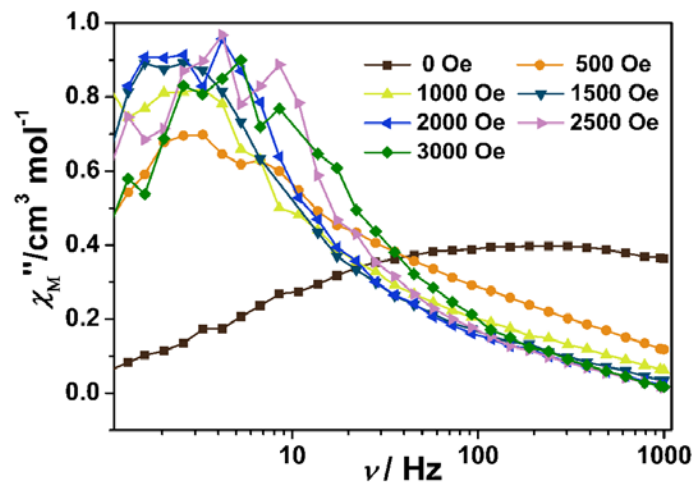
Figure S15. $\chi_M{'}$ and $\chi_M{''}$ versus ν plots (a), Cole-Cole plots (b) and $\ln(\tau)$ versus T^{-1} plot (c) for compound **α-Dy$_{0.10}$Y$_{0.90}$** under 2 kOe *dc* field. The solid lines are eye-guided (a) or best fits (b, c).
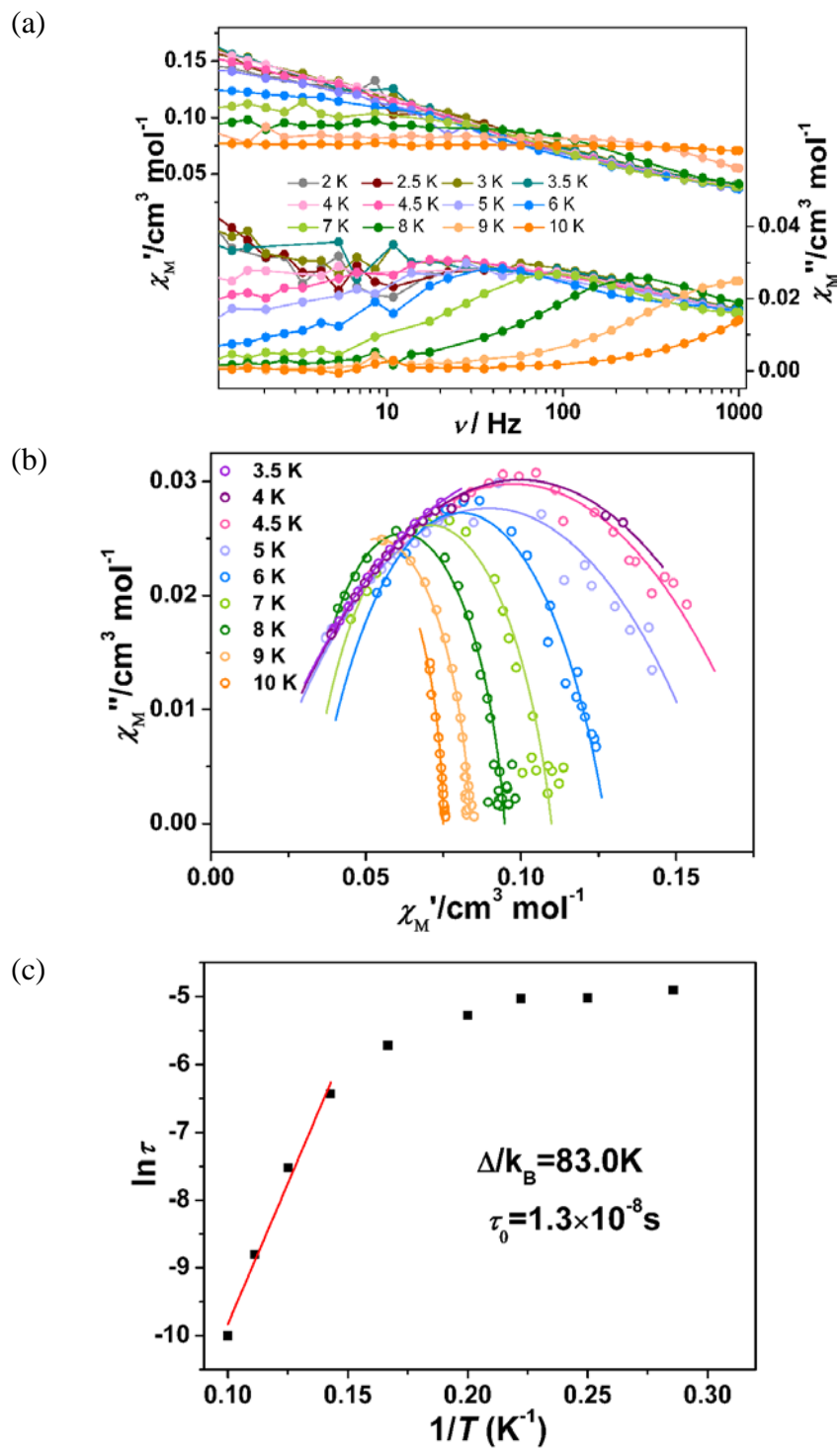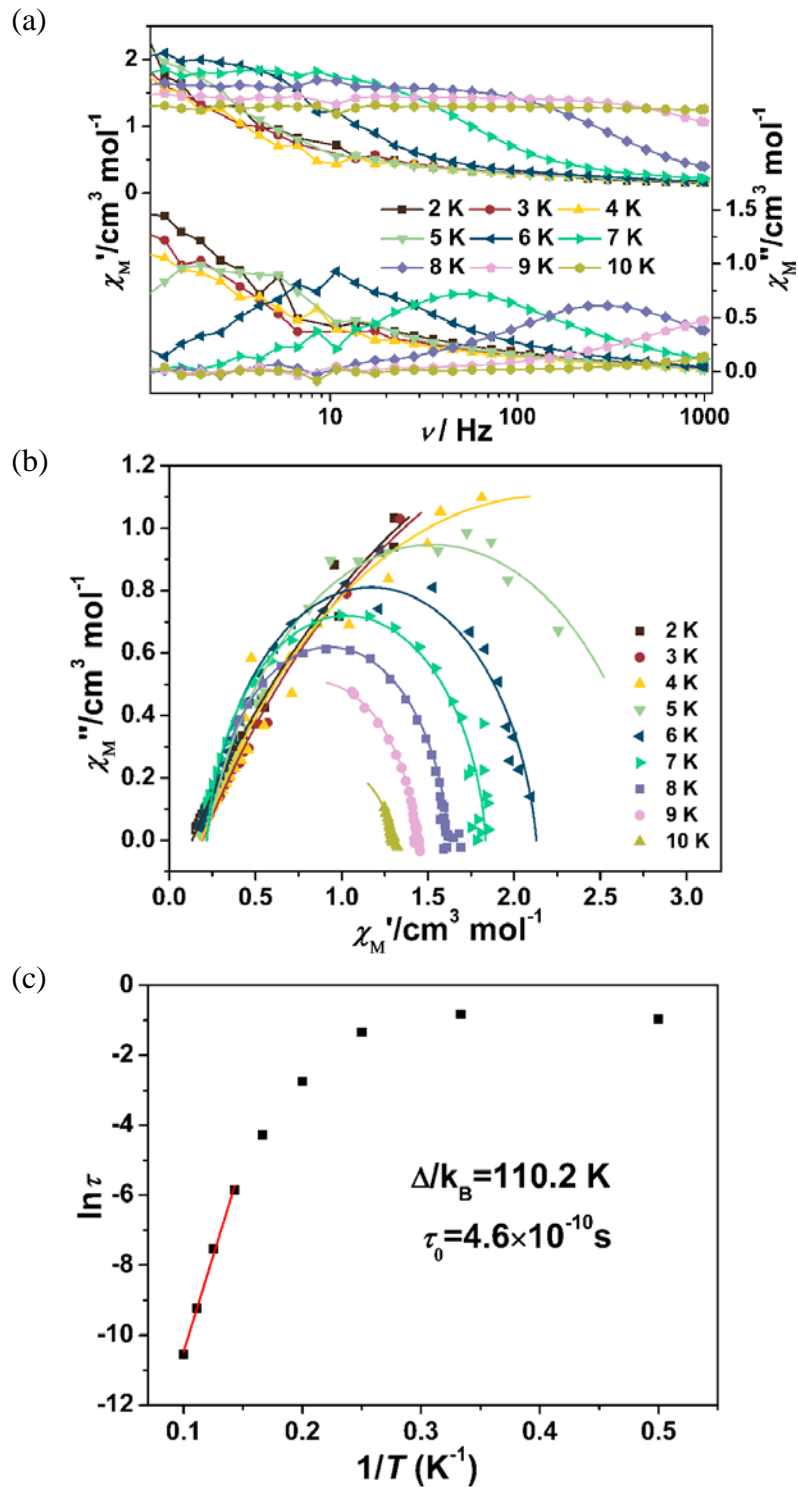
Figure S16. The χ_M' and χ_M'' versus frequency plots (a), Cole-Cole plots (b) and $\ln(\tau)$ versus T^{-1} plot for **β-Dy** under 2 kOe *dc* field. The solid lines are eye-guided (a) or best fits (b, c).
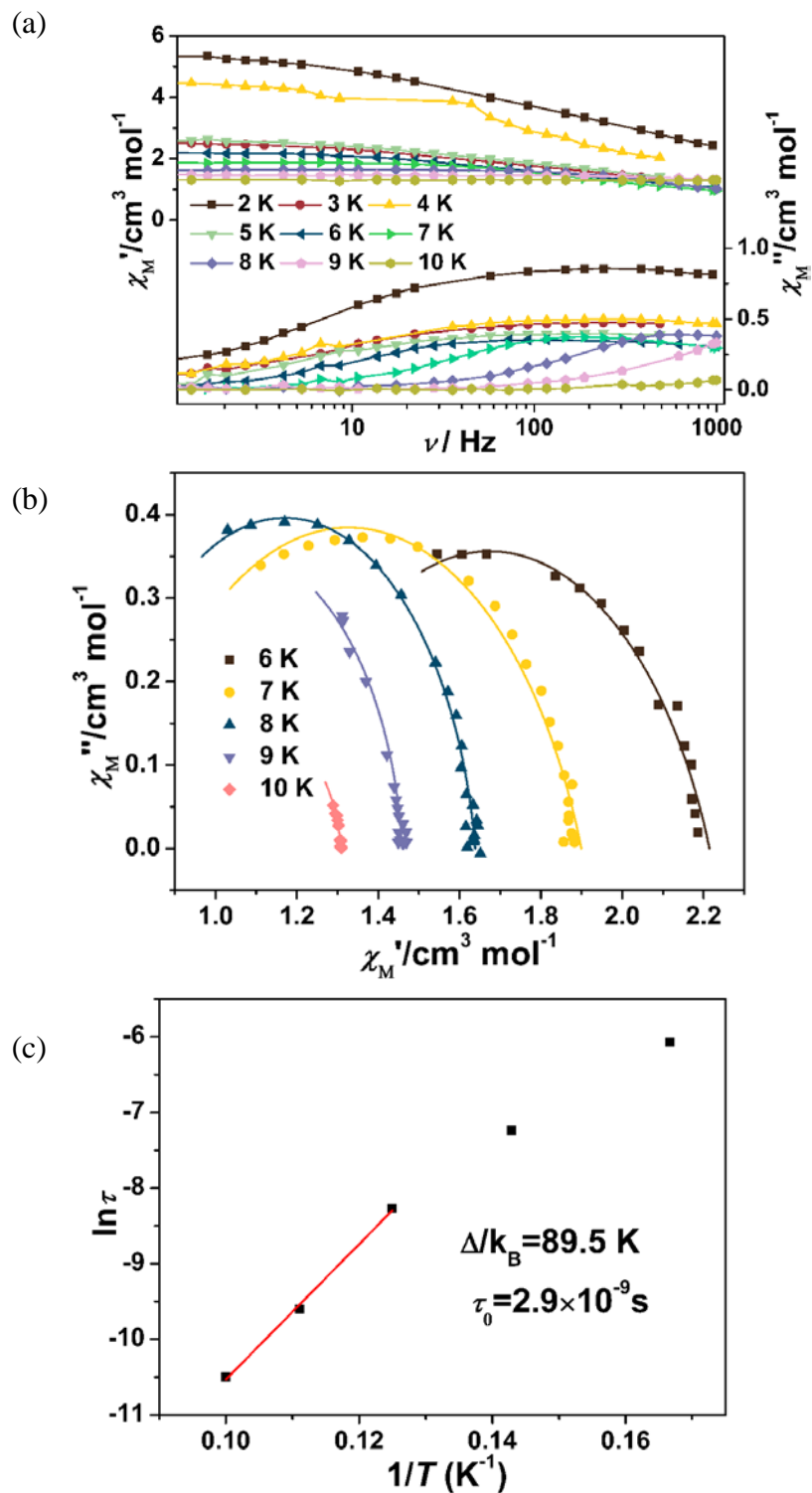
Figure S17. Frequency dependent in-phase (χ_M') and out-of-phase (χ_M'') signals (a), Cole-Cole plots (b) and the ln(τ) versus T^{-1} plot (c) for **β-Dy$_{0.12}$Y$_{0.88}$** at zero *dc* field. The solid lines are eye-guided (a) or best fits (b,c).

Figure S18. Frequency dependence of the out-of-phase susceptibility of **β-Dy$_{0.12}$Y$_{0.88}$** at 5 K under different dc fields.

Figure S19. Frequency dependent in-phase (χ_M') and out-of-phase (χ_M'') signals (a), Cole-Cole plots (b) and the ln(τ) versus T^{-1} plot (c) for **β-Dy$_{0.12}$Y$_{0.88}$** at 2 kOe *dc* field. The solid lines are eye-guided (a) or best fits (b,c).

(a)

(b)

(c)
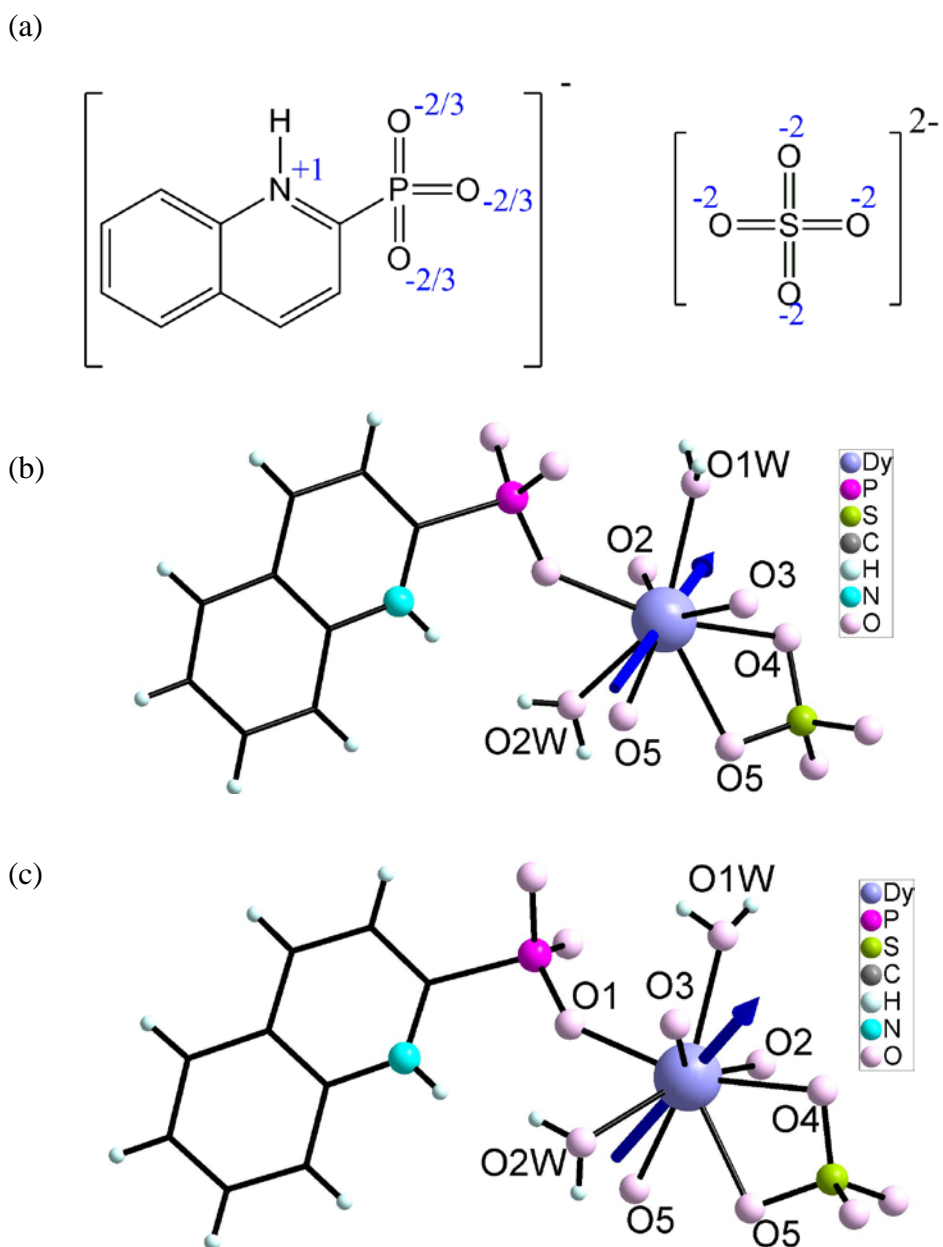
Figure S20. The orientation of the magnetic anisotropy is estimated by using MAGELLAN software. The 2-qpH$^-$ ligand, SO$_4{}^{2-}$ anion, five neighboring Dy^{3+} ions bridged via μ_3-O or O-P-O units are considered in the calculation. (a) The partial charges of the 2-qpH$^-$ and SO$_4{}^{2-}$ ligands; (b) The calculated easy-axis (blue arrow) in **α-Dy**; (c) The calculated easy-axis (blue arrow) in **β-Dy**. The direction of the arrow heads is arbitrary.